Resonant Raman spectroscopy of individual metallic and semiconducting single-wall carbon nanotubes under uniaxial strain

S. B. Cronin,[1,2] A. K. Swan,[3] M. S. Ünlü,[3,4] B. B. Goldberg,[3,4] M. S. Dresselhaus,[5,6] and M. Tinkham[2]
[1]*Department of Electrical Engineering — Electrophysics, University of Southern California, Los Angeles, California 90089, USA*
[2]*Department of Physics, Harvard University, Cambridge, Massachusetts 02138, USA*
[3]*Department of Electrical and Computer Engineering, Boston University, Boston, Massachusetts 02215, USA*
[4]*Department of Physics, Boston University, Boston, Massachusetts 02215, USA*
[5]*Department of Physics, Massachusetts Institute of Technology, Cambridge, Massachusetts 02139, USA*
[6]*Department of Electrical Engineering and Computer Science, Massachusetts Institute of Technology, Cambridge, Massachusetts 02139, USA*
(Received 14 February 2005; published 8 July 2005)

Uniaxial strain is induced by pushing single-wall carbon nanotubes (SWNTs) with an atomic force microscope tip. The vibrational and electronic energies of nanotubes are found to be very sensitive to strain. For both metallic and semiconducting SWNTs under strain, the D, G, and G' band Raman modes are downshifted by up to 27, 15, and 40 cm^{-1}, respectively. The relative strain-induced shifts of the D, G, and G' bands vary significantly from nanotube to nanotube, implying that there is a strong chirality dependence of the relative shifts. Semiconducting SWNTs remain strongly resonant under these large deformations, while metallic SWNTs appear to move in and out of resonance with strain, indicating a strain-induced shifting of the electronic subbands. Tight-binding calculations of the electronic band structure of semiconducting and metallic nanotubes under uniaxial strain predict significant shifting of the subband energies, leading to strain-induced changes in the Raman intensity. These theoretical predictions are consistent with what we observe experimentally for metallic nanotubes, but not for semiconducting nanotubes.

DOI: 10.1103/PhysRevB.72.035425 PACS number(s): 78.30.Na

I. INTRODUCTION

Resonant Raman spectroscopy is an excellent tool for studying single-walled carbon nanotubes (SWNTs). It provides a nondestructive way of measuring the precise phonon energies of nanotubes and requires relatively little sample preparation. When the laser energy is resonant with an electronic transition energy in a nanotube, the Raman signal can be large enough to observe spectra from an individual isolated SWNT.[1] Because of this resonance condition, Raman spectroscopy also gives a measure of the electronic band structure of the SWNTs.[1]

Many theoretical predictions have been made on the properties of individual SWNTs under strain.[2–5] These models predict significant changes in the electronic band structure and phonon frequencies under uniaxial strain. Evidence for these changes has been observed experimentally by measuring Raman spectroscopy of nanotube composite materials (such as nanotubes in epoxy) under strain.[6–9] However, these macroscopic Raman measurements are averaged over many SWNTs, both metallic and semiconducting, with different chiralities and different orientations and, hence, varying degrees of strain. The effect of strain is further complicated by the curing of the epoxy which causes a hydrostatic pressure-induced shift in the Raman modes[10] and also by fracture of the epoxy[11] which leads to an inhomogeneity of strain.

In this work we measure the direct effect of strain on *individual* SWNTs, thus eliminating effects of ensemble averaging and effects introduced by a composite medium. In our previous work[12] we demonstrated a large strain-induced downshift of the phonon frequency in two semiconducting nanotubes. In the current work we present data on 13 semiconducting nanotubes and 5 metallic nanotubes. We find that the strain-induced downshift of the phonon frequency depends strongly on chirality and that the radial breathing mode (RBM) Raman spectra of metallic nanotubes respond very differently to strain than those of the semiconducting nanotubes. The details and understanding of this difference will be discussed later in this paper.

II. EXPERIMENT

SWNTs synthesized by laser arc discharge are deposited from a sonicated dichloroethane solution onto a Si substrate coated by a 1-μm-thick layer of SiO_2. Metal pads of Cr -Au 1 μm wide are patterned on top of the SWNTs using electron beam lithography. A perpendicular displacement of the SWNT is created by pushing the SWNT with an atomic force microscope (AFM) tip,[14] as shown schematically in Fig. 1. The metal pads hold the ends of the SWNT in place, so the extra length added by the displacement creates a uniaxial strain. We determine the amount of strain in the SWNT by dividing the elongation [measured by subtracting the unstrained length from the deformed length in the AFM image of the SWNT (Fig. 1)] by the total unstrained length between the metal pads. This way any slack in the nanotube is accounted for in the prestrain length. This assumes that the strain is uniform along the length of the nanotube, an assumption justified by our spatially resolved Raman spectra.[12] Using this technique, we produce strains between 0.06% and 1.65%. Although the displacement of the nanotube is in the transverse direction, the resulting strain is primarily uniaxial.

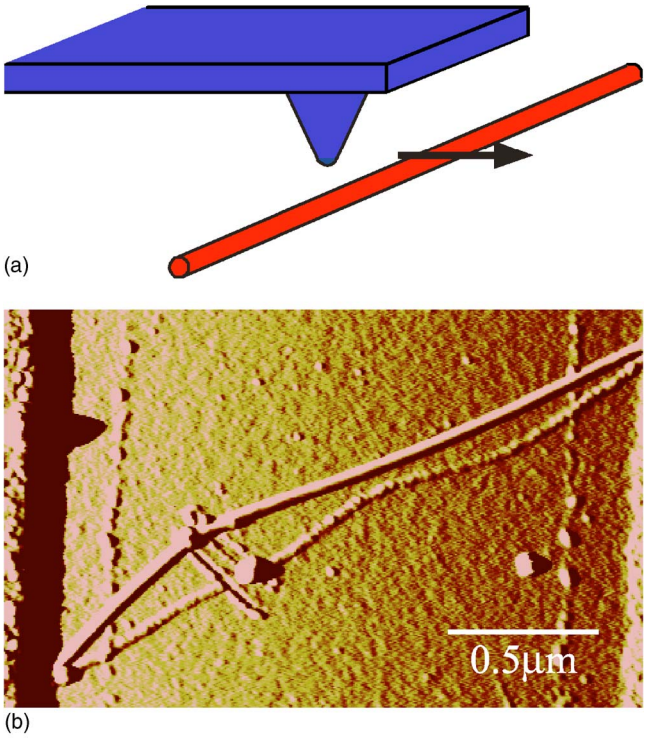

FIG. 1. (Color online) Top: schematic drawing of an AFM tip displacing a nanotube. Bottom: AFM image of a metallic SWNT held fixed at the ends by metal pads. The nanotube was strained by 0.95% with an AFM tip. Some residue remaining at the original position of the SWNT is visible in the AFM image and allows us to image the strained and unstrained lengths simultaneously.

Considering the large radius of curvature of the displacement (several microns) and the small radius of the nanotube (0.5 nm), we conclude that the transverse component of the strain is negligible. Therefore the elongation of the nanotube is the largest distortion to the lattice. Residue left over from lithographic processing can be seen in the AFM image of Fig. 1. Scratches in this residue layer can be seen where the AFM tip was dragged to displace the SWNT. The prestrained position of the SWNT can be seen easily because of the disturbance to the residue and this allows us to image the strained and unstrained lengths of the SWNT simultaneously. Raman spectra were measured on a Renishaw microprobe RM1000B with a 514-nm (2.41-eV) Ar-ion laser and a 633-nm (1.96-eV) HeNe laser. By aligning the laser spot relative to the metal pads, we can ensure from the AFM images that there is only one nanotube present. The average separation of nanotubes on these samples was $\sim 3-4$ μm. Spectra were taken at a laser power of 1–2 mW, with light polarized linearly along the nanotube axes.

III. UNIAXIAL STRAIN IN SEMICONDUCTING NANOTUBES

The SWNTs studied in this work have RBM frequencies in the range 170–194 cm^{-1}, which roughly correspond to a diameter range of 1.3–1.5 nm, obtained by using the relation $d_t = 248/\omega_{RBM}$.[1] By comparing the laser energy with the resonant transitions of all SWNTs within this diameter range calculated using a simple nearest-neighbor tight-binding model,[15,16] we determine that for this SWNT sample, the 514-nm (2.41-eV) Ar-ion laser is resonant with the third subband transition of semiconducting SWNTs, E_{33}^S.[17] The sharp characteristic G-band line shape corroborates the semiconducting nature of these SWNTs. Similarly, the SWNTs that are resonant with the 633-nm (1.96-eV) HeNe laser are metallic and resonant with the first subband transition E_{11}^M. These metallic SWNTs all exhibit a broad asymmetric Breit-Wigner-Fano (BWF) G-band line shape[18] corroborating their metallic nature.

TABLE I. Experimental downshifts of the D-, G-, and G'-band Raman-mode frequencies in cm^{-1} for semiconducting SWNTs resonant with a 514-nm Ar ion laser for various amounts of strain. Each row of data corresponds to data taken on the same SWNT. The different rows are for different nanotubes. The RBM frequencies are also given (in cm^{-1}) for nanotubes that exhibit this feature in their spectra.

Strain (%)	RBM	D band	G_- band	G_+ band	G' band
0.06	—	0.87	1.1	1.6	2.8
0.11	—	1.6	0.7	2.0	2.9
0.15	—	—	2.7	1.9	2.1
0.20	—	—	2.8	3.8	3.6
0.22	194	4.5	2.0	5.1	11.6
0.28	190	5.4	4.5	6.0	16.0
0.30	186	5.9	1.2	1.9	6.7
0.39	184	4.5	2.9	8.5	7.9
0.44	—	7.1	—	2.8	20.9
0.47	—	8.9	5.4	4.0	10.6
0.53	186	16.1	12.3	14.8	27.7
1.45	—	—	11.4	8.2	25.5
1.65	186	26.6	4.2	13.7	39.6

Looking first at the semiconducting nanotubes, we measured a total of 13 semiconducting SWNTs before and after inducing strain. We focus our study on the four main Raman features of SWNTs, the radial breathing mode (RBM) ($\sim 100-300$ cm^{-1}), the disorder-induced D band (~ 1320 cm^{-1}), the G band (~ 1590 cm^{-1}) with upper and lower frequency components G_+ and G_-, respectively, and the G' band (~ 2630 cm^{-1}). The downshift of the D, G, and G' bands is understood on the basis of the elongation of the carbon-carbon bonds, which weakens the bonds and therefore lowers their vibrational frequency. Typical Raman spectra for semiconducting nanotubes under strain are given in a previous publication.[12] The Raman peaks of the semiconducting SWNTs were fitted to Lorentzian line shapes, and the strain was estimated from the geometry of the nanotubes obtained from AFM images.

The results of these 13 semiconducting nanotubes are summarized in Table I and Fig. 2, where we have listed and plotted the strain-induced downshift of the D, G, and G' bands for all 13 semiconducting SWNTs. A consistent trend of increasing downshifts with increasing strain in these mode frequencies is apparent amidst the large spread in the data

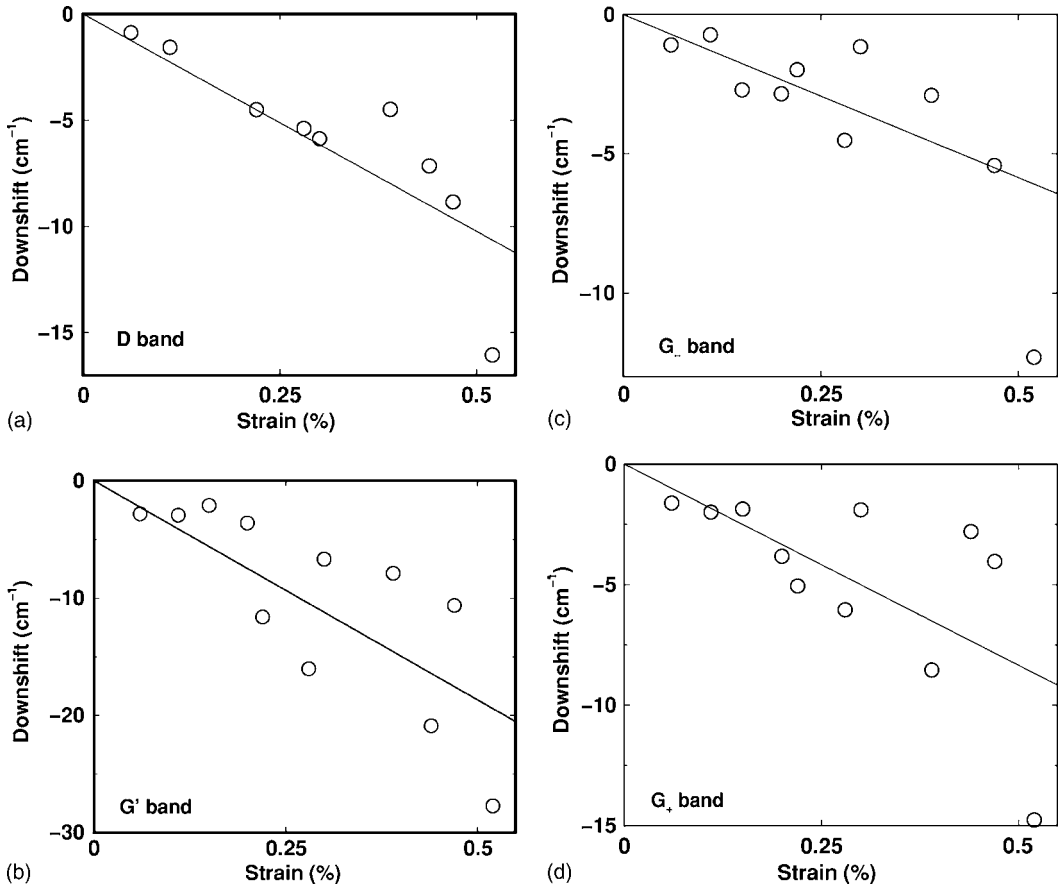

FIG. 2. Measured downshifts of the D-, G-, and G'-band Raman-mode frequencies of semiconducting SWNTs resonant with a 514-nm Ar ion laser plotted as a function of strain. Each point on a given plot was taken on a different SWNT.

points (see Fig. 2). The lines drawn in Fig. 2 represent least-squared error fits of 20.5, 11.7, 16.7, and 37.3 cm^{-1} per % strain for the D, G_-, G_+, and G' bands, respectively. To avoid having the large strain data points dominate the fit, the two data points corresponding to 1.45% and 1.65% strain were left out of the fit and Fig. 2. It is tempting to fit the G' and G^+ data in Fig. 2 to two lines, attributed to two families of behavior. However, the two families of points in G' do not correspond to the same nanotubes in the two families of G^+. It is also tempting to attribute the large spread in the data to our crude estimation of strain, perhaps made worse by slippage of the SWNTs under the metal electrodes. However, we should note that each point in these plots is taken from a different nanotube, and therefore, effects associated with diameter and chiral angle would be expected to lead to some variation. Each mode will depend on somewhat different force constants, which depend on chirality, so that for an individual SWNT, the large variability that is observed is not so unexpected. As is evident from Table I, the relative shifts of the D, G, and G' bands are not in a fixed relation with each other. That is, for some SWNTs the D band shifts more than the G band, while for other SWNTs the G band shifts more than the D band. We also observe a large variability in the relative shifts of the D and G' bands, and these relative shifts should scale roughly by a factor of 2, since $\omega_{G'} \approx 2\omega_D$ for unstrained SWNTs. We therefore conclude that a large variation in the strain dependence of the D, G, and G' modes exists for different nanotubes with different chiralities and is not an artifact of our determination of the strain.

The frequency downshifts observed are approximately 4 times larger than those observed in bulk composites.[6,7,9] This 75% underestimate of strain in these nanotube-epoxy composites is presumably due to slippage between the SWNTs and the epoxy matrix and to ensemble averaging errors. This result has some rather negative implications for applications where carbon nanotubes are added to a composite to increase the material's stiffness and strength, although some work on nanotube-polymer adhesion[13] indicates that adhesion is very strong. Therefore, the weak strain dependences observed in these composites may be due to poor nanotube dispersions.

For these semiconducting SWNTs, the RBM remained unchanged in both frequency and intensity under strain. This seemingly inconsistent result—that the D-, G-, and G'-band frequencies are strongly affected by strain while the RBM is unaffected—can be understood if we consider the large magnitude of the D-, G-, and G'-mode frequencies ($\sim$1320, 1590, and 2630 cm^{-1}) relative to the RBM ($\sim$190 cm^{-1}). The shifts observed in the D, G, and G' modes due to strain are approximately 1% of the mode frequencies. A 1% change in the RBM frequency would result in a less than 2 cm^{-1} shift, which is close to the minimum resolution of our spectrometer. For all six semiconducting nanotubes measured that showed a RBM feature in their spectra, no change in the RBM intensity or peak position due to strain was observed within our experimental accuracy.

It is surprising that the semiconducting SWNTs remain strongly resonant with the laser energy after such large perturbations to their lattice. This indicates that the positions of the van Hove singularities in the electronic band structure of the SWNT do not change significantly with strain. As calculated below, a strain of 1% can shift the band gap by as much as 100 meV. The range of laser energies over which the Raman signal of a nanotube can be observed is known as the resonance window. The resonance window of the RBM is expected to be ~60 meV.[19] We therefore expect to see a significant change in the intensity of the RBM for large strains. In addition, the relative intensity of the Stokes and anti-Stokes Raman peaks gives a very precise measure of the energy of a nanotube's van Hove singularities.[20] However, we observe no change in the Stokes/anti-Stokes intensity ratio in any of the six semiconducting SWNTs that showed a RBM feature in their spectra. This indicates that the strain-induced shift of the van Hove singularities (or electronic transition energies) does not exceed the resonance window. We do, however, see significant changes in the RBM intensity for metallic SWNTs, as will be discussed below.

IV. UNIAXIAL STRAIN IN METALLIC NANOTUBES

Raman spectra were also measured with a 633-nm (1.96-eV) HeNe laser which, for the diameter distribution of the SWNTs of this sample, are in resonance with predominantly metallic nanotubes. For these SWNTs the laser energy is in resonance with the first subband transition E_{11}^{M}. Figure 3 shows the Raman spectra of a typical metallic nanotube before and after inducing 0.95% strain. We see again significant downshifts of 10–15 cm^{-1} of the D-, G-, and G'-band Raman modes with strain, as we did for semiconducting SWNTs. The G band for metallic nanotubes looks quite different from that of semiconducting nanotubes. There is a sharp high-frequency component (G_{+}) that is also observed in the spectra of semiconducting nanotubes. However, the lower-frequency component (G_{BWF}) exhibits a broad asymmetric Breit-Wigner-Fano line shape associated with electron-phonon coupling to the continuum of electronic states in metallic nanotubes[18] and is not observed in semiconducting nanotubes.

In Fig. 3 we see that the RBM feature appears at 184 cm^{-1} after strain is induced, indicating that the SWNT was brought into better resonance with E_{laser} by the applied strain, while the intensities of the D, G, and G' bands change by only a fraction of the initial intensity. The shoulder peak appearing at 175 cm^{-1} originates from the underlying silicon substrate and will be ignored in our analysis. The D, G, and G' bands have larger resonance windows than the RBM because the RBM has a small phonon energy and therefore a smaller energy difference between incoming and outgoing photon resonance possibilities. This makes the RBM more sensitive to changes in the resonance condition,[19] either by changes in the laser energy or by changes in the energy of the resonant electronic transition in the SWNT. Since, in these experiments, the laser energy is fixed (1.96 eV), the change observed in the relative intensity of the RBM indicates a shift of the resonant transition E_{11}^{M}, such that E_{11}^{M} of the SWNT becomes closer to the laser energy. All five metallic SWNTs measured before and after strain showed significant changes in their RBM intensities. One SWNT was found to fall completely to an off-resonance situation after strain, while another was brought on resonance from a previously off-resonance situation. There were no observable differences in the intensities of the D, G, and G' bands for the nanotubes where strain improved the resonance condition relative to the nanotubes where strain spoiled the resonance.

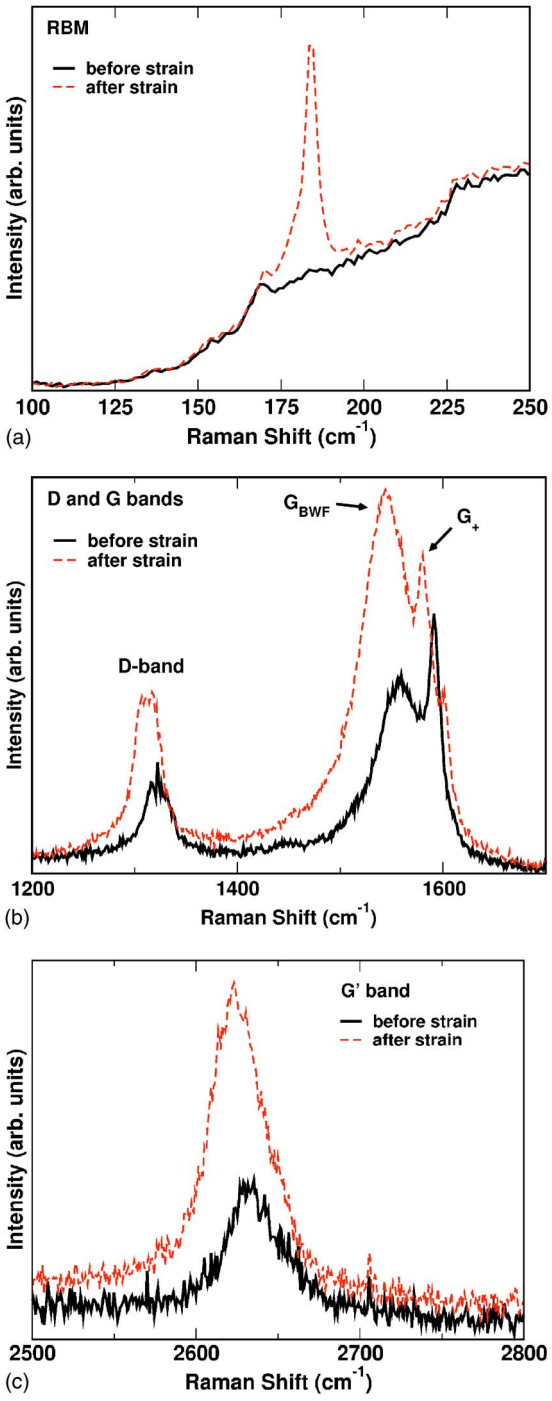

FIG. 3. (Color online) Raman spectra of the metallic SWNT of Fig. 1 measured with a 633-nm HeNe laser before and after inducing a 0.95% strain.

TABLE II. Downshifts of the D-, G-, and G'-band Raman-mode frequencies in cm^{-1} for metallic SWNTs resonant with a 633-nm HeNe laser for various amounts of strain. Each row corresponds to data taken on the same SWNT. The RBM frequencies are also given (in cm^{-1}), as well as the change in intensity of the RBM before and after strain.

Strain (%)	RBM	$\frac{I_{after}-I_{before}}{I_{before}}$	D band	G_{BWF} band	G_+ band	G' band
0.10%	180	139%	5.0	11.2	7.5	7.2
0.20%	188	−50%	12.6	10.5	11.7	−0.4
0.60%	193	89%	16.0	12.2	5.9	8.0
0.95%	184	∞	15.0	15.6	9.8	9.7
1.25%	170	−100%	21.4	14.6	—	38.0

Table II summarizes the Raman data of five metallic nanotubes measured before and after strain. The RBM and D-, G_+-, and G'-band peaks were fitted to Lorentzian line shapes, while the G_{BWF} was fit to a Breit-Wigner-Fano line shape.[18] The D, G, and G' modes are significantly downshifted to lower wave numbers when strain is applied. However, unlike semiconducting nanotubes the Raman mode shifts of metallic nanotubes do not seem to scale with strain, and there is considerable variability in the data. No change in the RBM frequency was observed; however, the intensity of the RBM was found to be very sensitive to strain.

The appearance and disappearance of the RBM with strain is in striking contrast to that of the semiconducting nanotubes, whose RBM's were not observed to change at all with strain. For metallic nanotubes the resonant electronic transition is between the first conduction and valence subbands E_{11}^M, whereas for semiconducting nanotubes the resonance is between the third subbands E_{33}^S. Detailed calculations of these two resonance conditions are discussed below.

V. TIGHT-BINDING CALCULATION

In order to understand the changes in the Raman intensity of nanotubes under strain we calculate the electronic subband energies using a tight-binding model similar to that developed by Yang *et al.*[3,8] The model is based on the nearest neighbor tight binding of two-dimensional graphite and the periodic boundary condition imposed by the quantization of the circumferential momentum k_c: namely, $k_c C_h a_0 = 2\pi j$, where j is an integer and C_h is the circumference of the nanotube in units of the graphene lattice vector $a_0 = 0.249$ nm. Under uniaxial strain ϵ, we allow the three C-C bond vectors to elongate in the axial direction:

$$\vec{r}_1 = \frac{a_0}{2}\frac{n+m}{C_h}\hat{c} + \frac{a_0}{2\sqrt{3}}\frac{n-m}{C_h}(1+\epsilon)\hat{t}, \tag{1}$$

$$\vec{r}_2 = -\frac{a_0}{2}\frac{m}{C_h}\hat{c} - \frac{a_0}{2\sqrt{3}}\frac{2n+m}{C_h}(1+\epsilon)\hat{t}, \tag{2}$$

$$\vec{r}_3 = -\frac{a_0}{2}\frac{n}{C_h}\hat{c} - \frac{a_0}{2\sqrt{3}}\frac{n+2m}{C_h}(1+\epsilon)\hat{t}, \tag{3}$$

where $\hat{c}$ and $\hat{t}$ are the circumferential and axial unit vectors, respectively. As the C-C bond length increases, we expect the overlap integral γ_0 to decrease inversely as the bond length squared,[3] $\gamma_i = \gamma_0 (r_0/r_i)^2$. The γ_0 value used in these calculations is 2.9 eV and the unstrained bond length r_0 is 0.144 nm. Including these strain-dependent terms in the tight-binding calculation gives the strain-dependent energy dispersion relations of carbon nanotubes:

$$E(\vec{k}) = \pm\{\gamma_1^2 + \gamma_2^2 + \gamma_3^2 + 2\gamma_1\gamma_2\cos[\vec{k}\cdot(\vec{r}_1 - \vec{r}_2)] + 2\gamma_1\gamma_3\cos[\vec{k}\cdot(\vec{r}_3 - \vec{r}_1)] + 2\gamma_2\gamma_3\cos[\vec{k}\cdot(\vec{r}_2 - \vec{r}_3)]\}^{1/2}.$$

Here the circumferential and axial components of the momentum are $k_c = 2\pi j/C_h a_0$ and $-\pi/T \leqslant k_t \leqslant \pi/T$, respectively, where T is the length of the unit cell. The density of states per unit length can be obtained from $E(\vec{k})$ by taking its derivative with respect to axial momentum and summing over the subbands:

$$\mathrm{DOS}(E) = \frac{1}{2\pi}\sum_{j=1}^{N}\left|\frac{dE_j(k_t)}{dk_t}\right|^{-1}, \tag{4}$$

where N is the total number of subbands. We should note that this model calculates the first-order perturbation of strain using a simple tight-binding model. It thus assumes that the energy eigenvalues do not mix and is expected to work well only for small perturbations in the low-strain limit.

We are interested in the strain dependences of the subband transition energies that are resonant with the laser energy, which for this experiment are E_{11}^M for metallic nanotubes and E_{33}^S for semiconducting nanotubes. Figure 4 shows the calculated joint density of states of a (14,6) semiconducting nanotube and a (16,1) metallic nanotube under 1% strain. Both nanotubes were chosen to have E_{ii} values similar to the laser energies used in the experiment (2.41 and 1.96 eV, respectively) and radial breathing mode frequencies (ω_{RBM}) similar to those observed in the experiments. Looking first at the (14,6) nanotube in Fig. 4, it is clear that 1% strain causes a downshift of 57 meV in the position of the van Hove singularity. For the (16,1) metallic nanotube in the figure, the two peaks of E_{11}^M shift toward each other by 94 and 76 meV due to the strain. Thus the application of 1% strain causes a decrease in the splitting of E_{11}^M by approximately 170 meV. These plots represent typical behavior under strain. However, for semiconducting nanotubes the position of the van Hove singularity can shift both upward in energy, if $(n-m)$ mod $3=1$, and downward, if $(n-m)$ mod $3=2$. These predictions are similar to those reported in Ref. 8.

Figure 5 shows the calculated shift of the subband transition energies plotted as a function of strain for various nanotubes with different chiralities. The strain-induced shifting of E_{11}^M (low energy component) and E_{33}^S is very linear in this strain range and is very sensitive to chiral angle. The shifting is largest for nanotubes with zero chiral angle (zigzag nanotubes) and smallest for nanotubes with large chiral angles. There is no shift for armchair nanotubes ($\theta = 30°$), whose

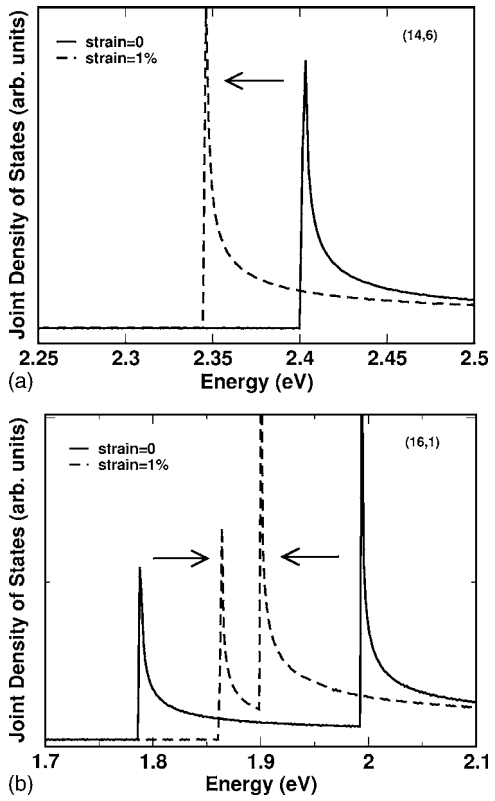

FIG. 4. Joint density of states for a (14,6) semiconducting nanotube and a (16,1) metallic nanotube with and without 1% uniaxial strain.

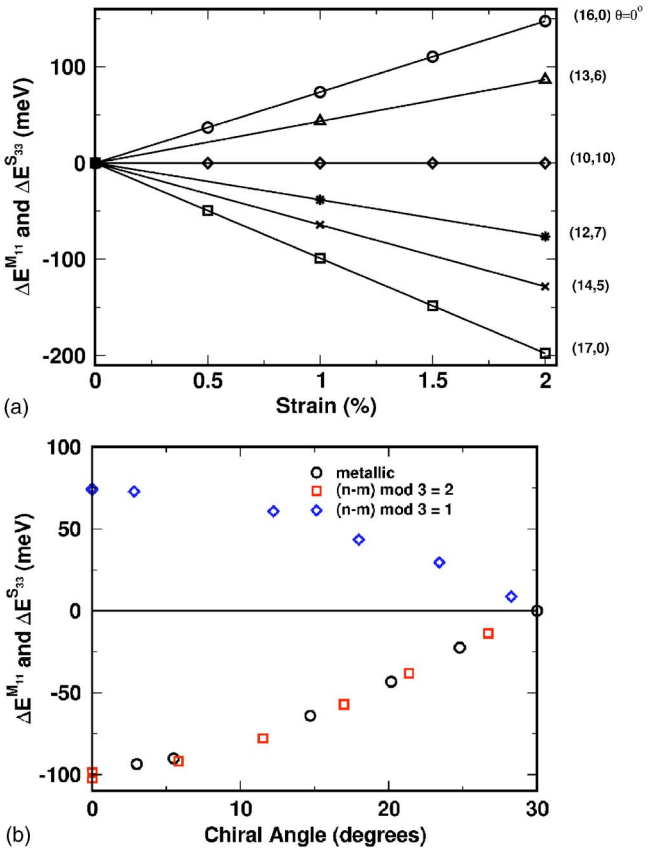

FIG. 5. (Color online) Top: calculated strain-induced shift of the intersubband transitions E_{11}^M and E_{33}^S. Bottom: chirality dependence of the shift in E_{11}^M and E_{33}^S under 1% uniaxial strain. Calculations were made on nanotubes in the diameter range 1.1–1.5 nm.

bonds make 30° and 90° angles with $\hat{t}$. The chiral angle dependences of the strain-induced shift of E_{33}^S and of the low-energy component of E_{11}^M at 1% strain are also plotted in Fig. 5. It is convenient to describe nanotubes under strain in $(n-m)$ mod 3 families. For $(n-m)$ mod 3=1, E_{33}^S increases with strain, and for $(n-m)$ mod 3=2, E_{33}^S decreases with strain. For E_{44}^S the strain-induced shifts are in the same direction as for E_{22}^S but opposite to E_{33}^S. For a given chiral angle, the shift in E_{33}^S for $(n-m)$ mod 3=1 semiconducting nanotubes is approximately 25% smaller in magnitude than those of the metallic nanotubes and of the $(n-m)$ mod 3=2 semiconducting nanotubes.

The intensity of the Raman signal is expected to change as the resonant subband transition energy shifts toward or away from the laser energy. The intensity of the resonant Raman signal can be expressed as

$$I(E_l) = \left| \int M \frac{g(E)dE}{(E_l - E - i\Gamma_r)(E_l \pm E_{ph} - E - i\Gamma_r)} \right|^2, \quad (5)$$

where M is the scattering matrix element which is assumed for simplicity to be constant in energy, $g(E)$ is the joint density of states, E_l is the laser energy, E_{ph} is the phonon energy, ~23 meV (185 cm^{-1}) for the nanotubes in this study, and Γ_r is the inverse scattering lifetime for the Raman scattering process.[19] The two terms in the denominator describe resonance conditions for incoming and outgoing scattered light. For the $\pm E_{ph}$ term, the $-$ sign applies to Stokes processes (phonon emission) and the + sign applies to anti-Stokes processes (phonon absorption).

Figure 6 shows the calculated intensity of the radial-breathing-mode Raman signal as a function of laser energy for a (14,6) semiconducting nanotube and a (16,1) metallic nanotube with and without strain. Here we plot both the high- and low-energy components of E_{11}^M, although only resonances with the low component have been observed experimentally for the RBM feature.[21] We see significant shifting of these resonant peaks due to strain. The peaks describe a resonance in the Raman intensity, which occurs when the laser energy is sufficiently close to the subband transition energy in the nanotube. The range of energies which yield a resonantly enhanced intensity is known as the resonance window and is approximately 60 meV. As can be seen from these plots, as the resonant peaks shift (due to strain) toward or away from the laser energy, the intensity can change by a large amount. The (14,6) nanotube represents a nanotube that shifts off resonance with applied strain, while the (16,1) nanotube shifts onto resonance with strain, like the experimentally measured SWNT of Fig. 3.

The strain-induced changes can either increase or decrease the Raman intensity, depending on the laser energy. The magnitude of the shift depends strongly on chiral angle, regardless of whether the nanotubes are semiconducting or metallic. From theory, we expect to see significant changes

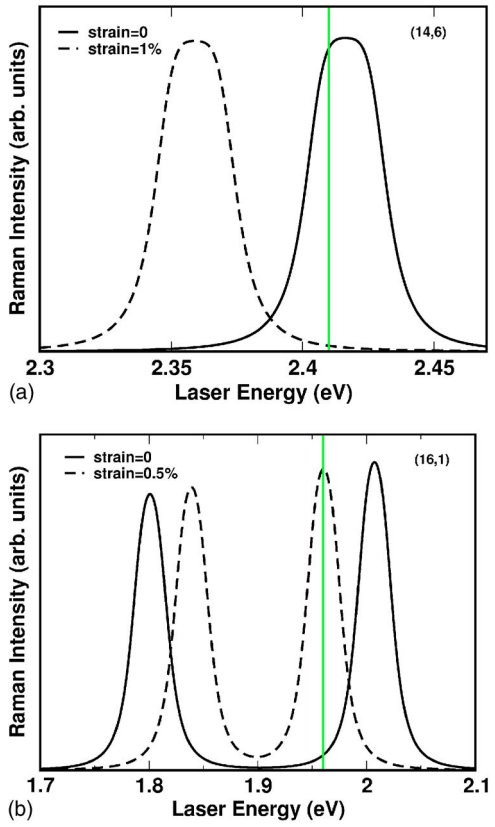

FIG. 6. (Color online) Raman intensity profiles for a (14,6) semiconducting nanotube and a (16,1) metallic nanotube calculated with and without uniaxial strain. The vertical lines indicate the fixed laser energies 2.41 eV, for semiconducting nanotubes, and 1.96 eV, for metallic nanotubes.

in the Raman intensity for both metallic and semiconducting nanotubes with small chiral angles ($\theta < 15°$). This is consistent with what we observe experimentally for metallic nanotubes. However, it is surprising that no such change is observed experimentally for the semiconducting nanotubes. One possible reason for this discrepancy between theory and experiment is that the semiconducting nanotubes may not be totally in resonance; therefore a large change in E_{ii} will not affect the intensity strongly. Another possible explanation is that the resonance window of the E_{33} transition of the semiconducting nanotubes is broadened by some additional factor not taken into account in the model calculation. A change in the RBM intensities of semiconducting nanotubes was obtained experimentally during the deformation of composites.[8] One difference is that a 785-nm laser was employed in that work, in resonance with the E_{22} transition of the nanotubes. In all of the work presented in this paper Raman spectra were taken at a fixed laser energy (514 and 633 nm). This technique could be further improved with a tunable laser whereby a shift in E_{ii} could be measured directly rather than by inferring it from the change in Raman intensity.

VI. CONCLUSIONS

Carbon nanotubes are found to be very sensitive to strain. By applying uniaxial strain we are essentially able to tune the electronic and vibrational energies of a single isolated nanotube in a controllable way. Raman spectroscopy is a very sensitive tool to study the effects of strain in carbon nanotubes. For uniaxial strains as low as 0.06% we can easily find resolvable shifts (>2 cm^{-1}) in the Raman frequencies. For metallic and semiconducting SWNTs with strain up to 1.65%, we find shifts in the D-, G-, and G'-band Raman-mode frequencies as large as 40 cm^{-1}. The relative shifts of the D, G, and G' bands with strain do not scale proportionally for different SWNTs and appear to be quite sensitive to chirality. For metallic SWNTs the observed RBM intensities vary with strain, which is attributed to the transition energy moving in and out of resonance as the applied strain is varied. Tight-binding calculations predict a strain-induced shifting of the subband transition energies of both semiconducting and metallic nanotubes. However, the RBM intensities of semiconducting nanotubes are not found to change with strain and may indicate that these nanotubes are not fully resonant with the laser energy.

ACKNOWLEDGMENTS

The authors would like to thank Shin Grace Chou and Eduardo Barros for helpful discussions. This research was supported in part by NSF Grant Nos. DMR-04-05538, DMR-02-44441, and NIRT ECS-0210752, NSEC Grant No. PHY-01-17795, and the Dupont-MIT Alliance.

[1] A. Jorio, R. Saito, J. H. Hafner, C. M. Lieber, M. Hunter, T. McClure, G. Dresselhaus, and M. S. Dresselhaus, Phys. Rev. Lett. **86**, 1118 (2001).
[2] R. Heyd, A. Charlier, and E. McRae, Phys. Rev. B **55**, 6820 (1997).
[3] L. Yang, M. P. Anantram, J. Han, and J. P. Lu, Phys. Rev. B **60**, 13874 (1999).
[4] T. Ito, K. Nishidate, M. Baba, and M. Hasegawa, Surf. Sci. **514**, 222 (2002).
[5] S. Ogata and Y. Shibutani, Phys. Rev. B **68**, 165409 (2003).
[6] C. A. Cooper, R. J. Young, and M. Halsall, Composites, Part A **32**, 401 (2001).
[7] V. G. Hadjiev, M. N. Iliev, S. Arepalli, P. Nikolaev, and B. S. Files, Appl. Phys. Lett. **78**, 3193 (2001).
[8] M. Lucas and R. J. Young, Phys. Rev. B **69**, 085405 (2004).
[9] M. D. Frogley, Q. Zhao, and H. D. Wagner, Phys. Rev. B **65**, 113413 (2002).
[10] J. R. Wood, M. D. Frogley, E. R. Meurs, A. D. Prins, T. Peijs, D. J. Dunstan, and H. D. Wagner, J. Phys. Chem. B **103**, 10388 (1999).
[11] P. M. Ajayan, L. S. Schadler, C. Giannaris, and A. Rubio, Adv. Mater. (Weinheim, Ger.) **12**, 750 (2000).

[12] S. B. Cronin, A. K. Swan, M. S. Ünlü, B. B. Goldberg, M. S. Dresselhaus, and M. Tinkham, Phys. Rev. Lett. **93**, 167401 (2004).

[13] A. H. Barber, S. R. Cohen, and H. D. Wagner, Appl. Phys. Lett. **82**, 4140 (2003).

[14] D. Bozovic, M. Bockrath, J. H. Hafner, C. M. Lieber, H. Park, and M. Tinkham, Phys. Rev. B **67**, 033407 (2003).

[15] R. Saito, G. Dresselhaus, and M. S. Dresselhaus, *Physical Properties of Carbon Nanotubes* (Imperial College Press, London, 1998).

[16] H. Kataura, Y. Kumazawa, Y. Maniwa, I. Umezu, S. Suzuki, Y. Ohtsuka, and Y. Achiba, Synth. Met. **103**, 2555 (1999).

[17] For nanotubes we write the electronic transitions in the form $E_{ij}^{M/S}$ for a transition from the ith valence subband to the jth conduction subband, and the metallic or semiconducting nature of the nanotube is indicated by the M or S superscript. In this paper we only consider $i=j$ transitions E_{ii}.

[18] S. D. M. Brown, A. Jorio, P. Corio, M. S. Dresselhaus, G. Dresselhaus, R. Saito, and K. Kneipp, Phys. Rev. B **63**, 155414 (2001).

[19] A. Jorio, A. G. Souza Filho, G. Dresselhaus, M. S. Dresselhaus, R. Saito, J. H. Hafner, C. M. Lieber, F. M. Matinaga, M. S. S. Dantas, and M. A. Pimenta, Phys. Rev. B **63**, 245416 (2001).

[20] A. G. Souza Filho, A. Jorio, J. H. Hafner, C. M. Lieber, R. Saito, M. A. Pimenta, G. Dresselhaus, and M. S. Dresselhaus, Phys. Rev. B **63**, 241404(R) (2001).

[21] C. Fantini, A. Jorio, M. Souza, M. S. Strano, M. S. Dresselhaus, and M. A. Pimenta, Phys. Rev. Lett. **93**, 147406 (2004).